Comparison of the structural, electrical, and optical properties of amorphous silicon-germanium alloys produced from hydrides and fluorides

K. D. Mackenzie,* J. H. Burnett, J. R. Eggert,† Y. M. Li, and W. Paul
Division of Applied Sciences and Department of Physics, Harvard University, Cambridge, Massachusetts 02138
(Received 28 January 1988; revised manuscript received 12 May 1988)

Amorphous silicon-germanium alloys have been prepared in the same rf glow-discharge reactor from ($SiH_4 + GeH_4$) and ($SiF_4 + GeF_4 + H_2$) mixtures at substrate temperatures between 200 and 400 °C. The principal aim of the investigation has been to discover whether preparation of these alloys from fluorides rather than from hydrides will result in better photoelectronic properties, and if so, whether the underlying cause is the substitution of fluorine for hydrogen in the alloy, or some other structure-related alteration of the material. Thus the apparatus, preparation procedures, characterizational techniques, and property measurements follow those of an earlier publication on alloys produced from hydrides alone. The only significant difference in photoelectronic properties found has been an order-of-magnitude improvement of the photoconductivity of alloys with band gaps near 1.5 eV. Evidence is assembled to assert that fluorine substitution for hydrogen in the alloy is not the cause of the changes in photoelectronic properties, but that these are more probably related to changes in a two-phase heterostructure, which are revealed most directly by transmission electron microscopy. A two-phase, two-transport-path model is proposed to explain the improved photoconductivity obtained with the fluoride-derived alloys.

I. INTRODUCTION

Hydrogenated amorphous silicon (*a*-Si:H) is presently much investigated as a material suitable for solar cell, electrophotographic, and vidicon applications.[1] For all of these structures, it would be advantageous to have a semiconductor of band gap somewhat smaller than *a*-Si:H (e.g., 1.5 eV rather than 1.8 eV) but with substantially the same photoelectronic response as measured, for example, by the mobility-lifetime products for photoelectrons and holes. Alloying Ge with Si (*a*-$Si_{1-x}Ge_x$:H) gives a material of suitably reduced band gap, but it is universally found, independent of the method of preparation, that the photoelectronic response is considerably poorer. In an earlier publication,[2] we reviewed the literature on this subject up to September 1984, and reported on our own systematic and extensive investigation of *a*-$Si_{1-x}Ge_x$:H alloys prepared under a variety of conditions over the full composition range. In that paper we described the results of measurements as a function of x of dc conductivity, photoconductivity, optical and ir absorption, photoluminescence, and transmission electron microscopy, and discussed possible reasons for the changes in properties, based on a suggested band structure for the alloys and on the occurrence of increased heterostructure in the films with increasing x.

Since 1983, several research groups[3–6] have followed up on the discovery by Nozawa *et al.*[7] that preparation by glow discharge of silicon-germanium alloys from mixtures of fluorides and hydrogen ($SiF_4+GeF_4+H_2$) improved the photoconductivity of alloys of band gap near 1.5 eV by about an order of magnitude. This work was based, at least in part, on the pioneering investigation by Madan *et al.*[8] of the properties of *a*-Si:H:F and a speculation[9] that F might be a better bond terminator *in the alloys* than in unalloyed Si. The investigation reported here concentrates primarily on the preparation of 1.4–1.5-eV band-gap *a*-$Si_{1-x}Ge_x$:H:F ($x=0.3-0.5$) by rf glow discharge of mixtures of ($SiF_4+GeF_4+H_2$), in the same reactor as our earlier work on *a*-$Si_{1-x}Ge_x$:H,[2] and a detailed comparison of the structural, electrical, and optical properties of the two alloy preparations.[6,10–12] We have found that the differences in the electrical and optical properties, and by inference the electronic band structure, are minor (although not insignificant), with the sole exception of the photoconductivity response, which can be improved by up to an order of magnitude.[7] From examination of the properties of F in the alloys (infrared absorption spectra, Raman spectra, electron microprobe) we conclude that substitution of F for H cannot be responsible for the improved photoresponse. From a transmission electron microscope examination of alloys produced from the hydrides and the fluorides, we conclude that the two-phase microstructure is different on a scale of 5–20 nm, and we infer that this probably affects phototransport more than it does optical absorption, photoluminescence, or electronic band structure. We adduce preliminary and less direct supporting evidence from studies of the infrared absorption spectra and deuteron magnetic resonance.[13] It is shown that a simple model based on two-phase microstructure is adequate to explain the difference in phototransport in the two alloy preparations.[11]

While this study focuses attention on the differences in microstructure between hydride- and fluoride-produced material as the cause of improved photoresponse in the

latter, it also confirms that the changed constitution of the microstructure is responsible, at least in part, for the deterioration of the photoelectronic properties of amorphous Si-Ge alloys, howsoever prepared, from those of *a*-Si:H.[2] The study leaves unaffected our earlier conclusion[2] that the different density-of-states distributions in all Si-based alloys (of larger or smaller band gap), based primarily on differences in the energy of dangling-bond states, are likely to lead to a degradation in the photoresponse. Finally, although our present study has confirmed[7] that the use of fluorides plus hydrogen can give material of improved photoresponse, we point out that other gas mixtures not involving fluorides have recently also given good photoresponses.[14] To some extent, the conclusions to be drawn from these recent studies are uncertain where the energy of the Fermi level has not been reported, but viewed overall, they suggest the necessity for more detailed examination of the structure of the alloys and its relation to the totality of conditions in the preparation plasma and at the film growth surface.

II. APPARATUS AND PROCEDURE

In our earlier paper[2] we discussed in detail our glow-discharge reactor, the method of sample deposition, and the characterization and measurement of properties of the samples. Here we shall discuss only the changes necessary in preparing *a*-$Si_{1-x}Ge_x$:H:F from mixtures of ($SiF_4+GeF_4+H_2$). The SiF_4 and GeF_4 were both of 99.99% purity and the H_2 of 99.999% purity.[15] The composition x depends very differently on the ratio of GeF_4 to SiF_4, and on the rf power, than it does on the ratio of GeH_4 to SiH_4, and the rf power, in the preparation of *a*-$Si_{1-x}Ge_x$:H. We conclude that GeF_4 molecules are much more easily dissociated than either SiF_4 or H_2. Thus low rf power results in Ge-rich films with poor photoelectronic properties. Based on such studies, the following conditions were adopted to produce alloys with $x \approx 0.5$: rf power density of 430 mW/cm^2, total pressure of 0.41 torr, and flow rates of 34.8 cm^3/min at STP (SCCM) for SiF_4, 0.7 SCCM for GeF_4, and 6.0 to 15.0 SCCM for H_2. Minor adjustment of the GeF_4 flow rate gives alloys of different x. While the power densities used are an order of magnitude greater than in the preparation of *a*-$Si_{1-x}Ge_x$:H, the deposition rates are approximately the same, i.e., 1–3 Å/s.

In contrast to our production of *a*-$Si_{1-x}Ge_x$:H from hydrides, the composition (x) of our $Si_{1-x}Ge_x$:H:F films varies across the 10-cm-diameter substrate platform. This resulted very probably from the low ratio of GeF_4 to SiF_4 in the gas mixture and from the slightly asymmetric arrangement for the introduction of the reactant gases. For a typical set of deposition parameters, the Ge content x varies from 0.3 to 0.5 on the substrate platform and by ± 0.01 over a typical substrate dimension of about 1 cm. The Ge content variation across the platform is far greater than in our production from hydrides (there the variation is not detectable on the scale of the estimated 1% accuracy of our electron microprobe composition determination). However, in an extensive series of tests, we have found that the variation is very reproducible from run to run. Our usual procedure is to codeposit a number of samples for different property measurements. A sample for a particular property measurement is always taken from a predetermined location on the substrate platform. This, combined with our procedure of measuring composition (whenever practicable) on the actual film whose property is being measured, has permitted us to determine systematically the changes in properties with x.

The properties measured on the alloys included electron microprobe analysis of the Si, Ge, and F contents, secondary-ion mass spectroscopy (SIMS) analysis of the impurity distribution in selected films, infrared vibrational spectra from which the H and F content and configuration could be inferred, transmission electron microscopic (TEM) examination of 50-nm-thick films on C-coated Ni microgrids, electrical conductivity measurements between room temperature and 475 K, optical absorption spectra in the visible and near infrared regions, photoconductivity spectra between 0.8 and 1.5 eV from which absorption spectra could be inferred, transient photoconductivity by the time-of-flight (TOF) method using a sandwich configuration to determine electron drift mobilities μ and electron-drift-mobility–lifetime ($\mu\tau$) products and also details on the conduction-band tail,[10–12,16,17] photoluminescence spectra at 77 K, Raman spectra, space-charge-limited current (SCLC) measurements on n^+-*i*-n^+ sandwich structures,[18] electron spin resonance determination[19] of neutral dangling bond densities, and measurements of deuteron magnetic resonance.[13] The details of the majority of the experimental techniques have already been given[2] and need not be repeated here.

III. CHEMICAL COMPOSITION OF FILMS PRODUCED FROM HYDRIDES AND FLUORIDES

The rf glow-discharge apparatus[20] was constructed and operated so as to minimize the incorporation of unwanted species such as O. The base vacuum was 3×10^{-8} torr, the gases were the purest available, and a residual gas analyzer was used periodically to monitor the gas mixture in the reactor. On selected films SIMS measurements[21] were made. Figure 1 shows the spatial distribution of the principal elements, but not their absolute concentration, as that requires calibration factors which are not reliable. It is clear that the spatial distribution is uniform over most of the film.

An electron microprobe[22] was used to determine the atomic concentration of Si, Ge, and F. The concentration of F was of the order of 1 at. % in all of the films produced from fluorine-containing gases. The concentration of H was estimated from the area under the wagging mode of the infrared vibrational absorption spectra; as an example, it was of the order of 5 at. % for a 50:50 alloy, whether prepared from hydrides or fluorides. No attempt was made to determine the concentration of H more accurately by other techniques, as it is our observation that films of good photoelectronic properties can have a wide range of acceptable concentrations of H, so that only a very low atomic percentage (say, less than

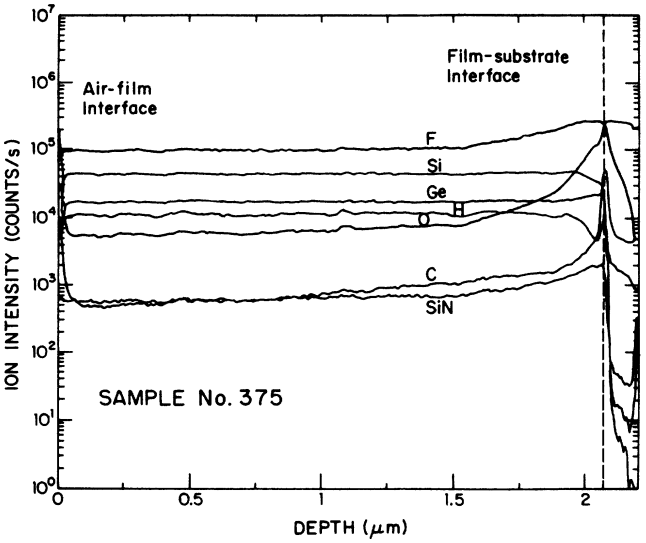

FIG. 1. SIMS depth profile of an a-$Si_{1-x}Ge_x$:H:F alloy. The Ge and F contents as determined from electron microprobe are 41 and ~1 at. %, respectively.

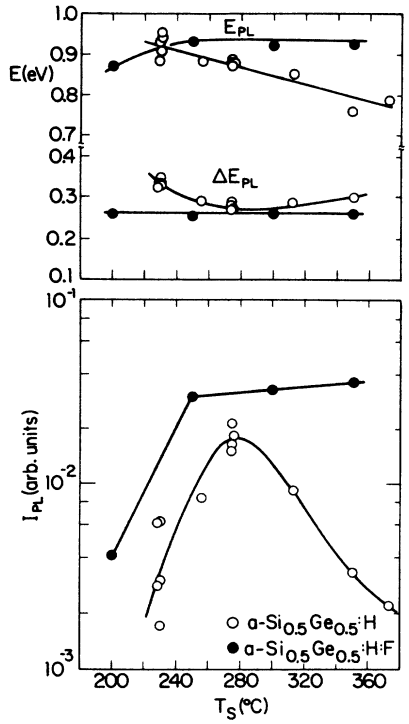

FIG. 2. E_{PL}, ΔE_{PL}, and I_{PL} versus T_s for a-$Si_{0.5}Ge_{0.5}$ samples prepared from hydrides and fluorides.

2–3 %) or a very high atomic percentage (say, larger than 15%) merits special concern. Of course, a large *variation* in the concentration of H among different films (which did not occur) implies changes in many other material properties, including the energy gap. The configuration of bonded H in the films, as revealed by the details of the stretching vibrational absorption (the occurrence of 2090-cm^{-1} Si—H and 1975-cm^{-1} Ge—H modes) and the presence of bending modes (between 800 and 900 cm^{-1}) is regarded as a more significant indicator of film quality than the absolute concentration of H.

IV. VARIATION WITH T_s OF THE PROPERTIES OF a-$Si_{0.5}Ge_{0.5}$:H AND a-$Si_{0.5}Ge_{0.5}$:H:F

In our earlier paper,[2] we discussed the variation of the optical energy gap, the photon energy of the maximum photoluminescence, the intensity of the peak in photoluminescence, the magnitude of the photoconductivity at 1.96 eV, and the hydrogen content as a function of deposition temperatures T_s between 200 and 400 °C. We concluded that all of the results could be explained as a competition between two effects of increase in T_s: increased healing of defects and disorder, and decreased incorporation of H in the film. A similar but less extensive study was carried out for the fluoride-derived samples. As observed previously for hydride-derived a-$Si_{0.5}Ge_{0.5}$, the hydrogen content decreases monotonically with increasing T_s. However, the decrease is much less. For example, the hydrogen content changes from about 7 at. % at T_s of 200 °C to about 4 at. % at 350 °C compared to a change from about 13 at. % at T_s of 230 °C to about 4 at. % at 350 °C. The optical gap is essentially independent of T_s in contrast to our results for a-$Si_{0.5}Ge_{0.5}$:H that indicated a linear decrease in gap with increasing T_s. Significantly different results were obtained for the photoluminescence (PL). Figure 2 shows the variation of the energy E_{PL}, the full width at half maximum (FWHM) ΔE_{PL}, and the intensity I_{PL} of the photoluminescence peak for a series of a-$Si_{0.5}Ge_{0.5}$:H:F alloys for T_s between 200 and 350 °C, and compares them with those for a-$Si_{0.5}Ge_{0.5}$:H produced in the same system from SiH_4+GeH_4. All PL measurements were done at 77 K using 2.41-eV excitation following our standard procedure.[23] Based on the near-constancy of the PL parameters for the fluoride-derived samples near and above 300 °C, and the fact that $T_s=300$ °C optimized the photoconductivity and photoluminescence of the hydride-derived films, we adopted a T_s of 300 °C for the bulk of our measurements on the fluoride-derived alloys. We postpone further comment on the details of Fig. 2 to the Discussion section.

V. VARIATION WITH x OF THE ELECTRICAL AND OPTICAL PROPERTIES OF a-$Si_{1-x}Ge_x$:H AND a-$Si_{1-x}Ge_x$:H:F

Figure 3 compares the optical absorption edges of a-$Si_{1-x}Ge_x$:H and a-$Si_{1-x}Ge_x$:H:F. Between $h\nu=0.8$ and roughly 1.5 eV, the spectra are deduced from the spectra of photoconductivity using the constant photocurrent method.[24] The photoconductivity-derived part of the absorption spectrum is normalized to the part from direct optical transmission measurements in the range of overlap at higher photon energies near an α of 10^3 cm^{-1}. We shall not address here legitimate questions that arise concerning the derivation of an absorption spectrum from a photoconductivity spectrum, since the significant fact for our present purpose is that the spectra for hydride- and

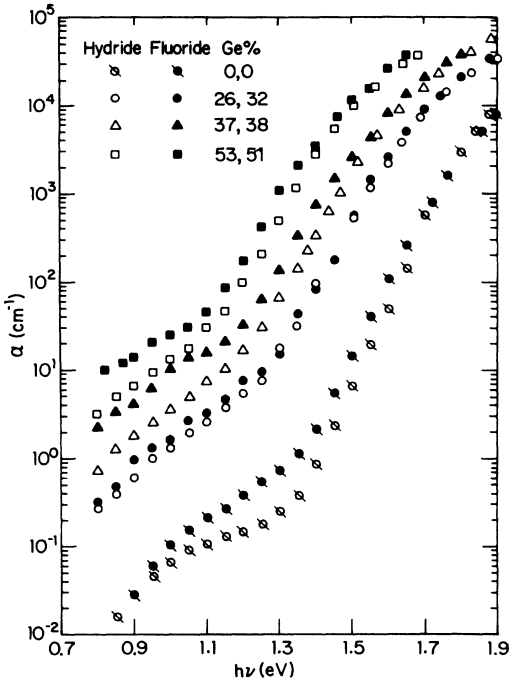

FIG. 3. Optical absorption spectra for a-$Si_{1-x}Ge_x$ alloys produced from hydrides and fluorides.

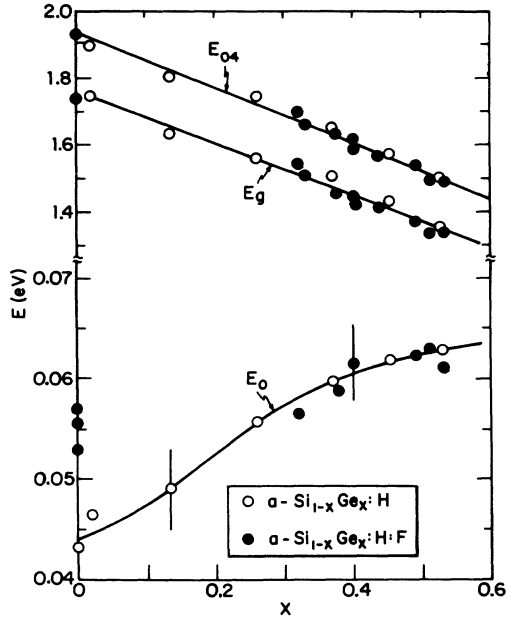

FIG. 4. Variation of E_{04}, E_g, and E_0 with x.

fluoride-derived material of similar x practically coincide. From such absorption edges, we deduce three parameters: (1) the energy gap E_g, derived from the extrapolation of the part of the edge above 10^3 cm^{-1} to zero absorption coefficient using the formula[25]

$$(\alpha h\nu)^{1/2}=A(h\nu-E_g)\ ;$$

(2) the energy E_{04}, the photon energy at which $\alpha=10^4$ cm^{-1}, which is also a conventional measure of the energy gap; and (3) the energy E_0, the so-called Urbach parameter in the exponential region of the edge, derived from the formula

$$\alpha=B\exp\left[\frac{h\nu-E_g}{E_0}\right].$$

Figure 4 shows the variation with x of E_g, E_{04}, and E_0. The variations of E_g and E_{04} are identical for the two types of material. E_g follows the empirical relation $E_g=1.76-0.78x$. If one excludes the points for $x=0$ for the fluoride-derived material (where there was no attempt to optimize preparation conditions) then the Urbach parameter E_0 is the same for the two preparations for $0.2<x<0.6$.

In Figure 3 the sub-band-gap absorption ($h\nu<1.4$ eV) is the same for $x\approx0.3$ for the two preparations of material. For other values of x, the values of α at photon energies about 0.5 eV below the absorption edge are always comparable for the two preparations; for example, for $x\approx0.5$ the values of α at $h\nu=0.9$ eV are 7 cm^{-1} for the hydride-derived and 14 cm^{-1} for the fluoride-derived films.

Figure 5 illustrates the dependence on x of two PL parameters for the two preparations of material.[26] The variations of I_{PL} with x are virtually identical, but those of ΔE_{PL} are quite different: there is considerable scatter in the values but the FWHM is consistently smaller in the fluoride-derived material. Examination of the spectra for these fluoride-derived samples, as well as for the hydride samples previously reported, shows no evidence for a "universal low energy tail" as reported by Gal *et al.*[27] In recent work of Street *et al.*[28] on a-$Si_{1-x}Ge_x$:H, such a tail is observed but only for a small group of the total samples investigated.

Figure 6 shows representative data of activated dark conductivity σ versus inverse temperature for samples with $x\approx0.5$ prepared from the different gas mixtures. All specimens were heated under vacuum to about 200 °C for 30 min before the measurements were performed, in order to ensure that any photoproduced defects were annealed out.[29] In all transport measurements, checks were made for a linear variation of current with the voltages used. The conductivity is given by the expression

$$\sigma=\sigma_{00}\exp[(E_f-E_c)/kT]\ .$$

If we use the approximate (but usual) description

$$E_f-E_c=(E_f-E_c)_0+\gamma T\ ,$$

then

$$\sigma=\sigma_{00}\exp\left[\frac{\gamma}{k}\right]\exp\left[\frac{(E_f-E_c)_0}{kT}\right].$$

We then focus on the dependence on x and preparation plasma of three parameters or observables (1) the activation energy $E_\sigma=(E_c-E_f)_0$; (2) the pre-exponential

$\sigma_0=\sigma_{00}\exp(\gamma/k)$, where σ_{00} is a function of conduction-band state density, temperature, and band mobility; and (3) the occurrence of a downward kink in $\log_{10}\sigma$ versus $1/T$ at high temperatures. In Fig. 6, this is seen to occur near $10^3/T=2.3\ \mathrm{K}^{-1}$; it must be emphasized that such a kink is a long-studied feature seen in many of the amorphous silicon and germanium films, both hydrogenated and unhydrogenated, and not an artifact of our apparatus or procedure.[30] Practically all of the alloys, whether grown with fluorine present or not, show a downward kink in $\log_{10}\sigma$ versus $10^3/T$ for $10^3/T \leq 2.3\ \mathrm{K}^{-1}$.

Figure 7 compares the variation of σ_0 with E_σ (a "Meyer-Neldel[31] plot") for alloys with a range of x values produced from the two different gas mixtures. While this variation is linear, inside of scatter, for a-$Si_{1-x}Ge_x$:H, that for a-$Si_{1-x}Ge_x$:H:F divides into two groups which straddle the data for a-$Si_{1-x}Ge_x$:H.

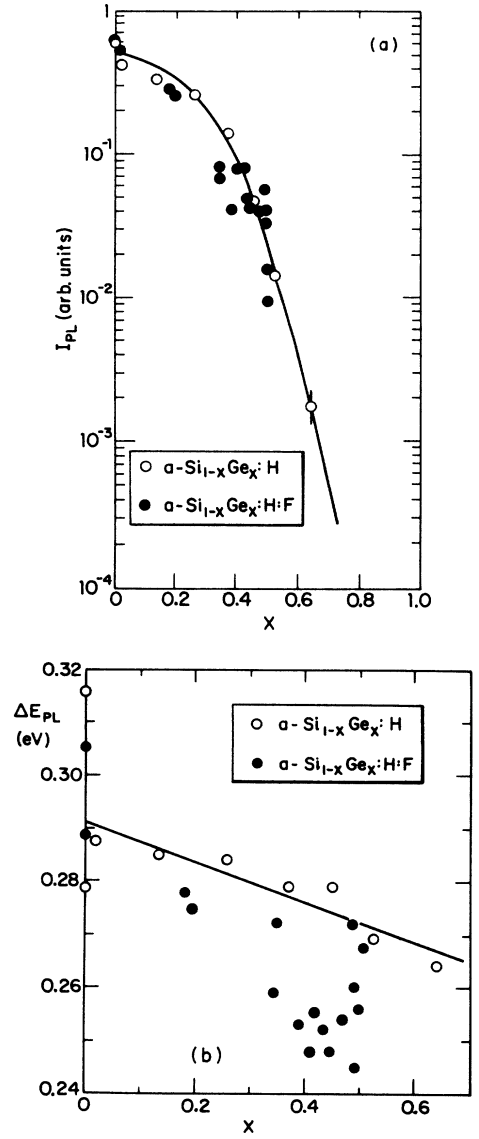

FIG. 5. Variation of (a) I_{PL} and (b) ΔE_{PL} with x.

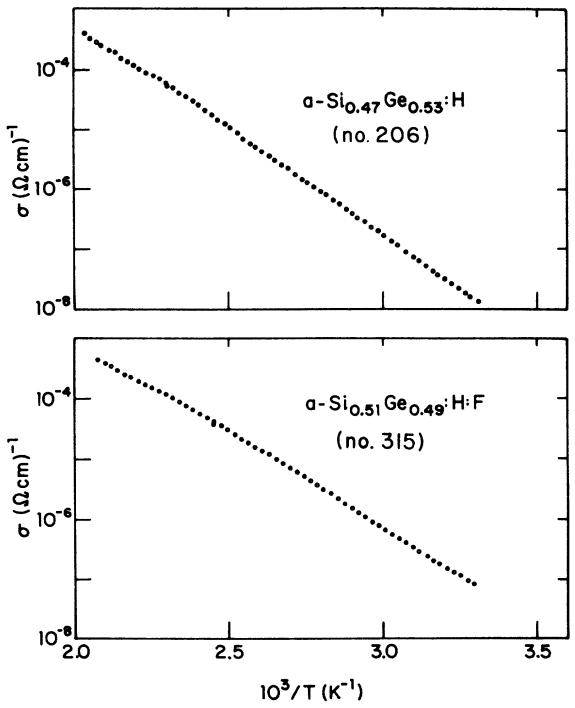

FIG. 6. Dark conductivity σ versus inverse temperature for a-$Si_{0.5}Ge_{0.5}$ produced from hydrides and fluorides.

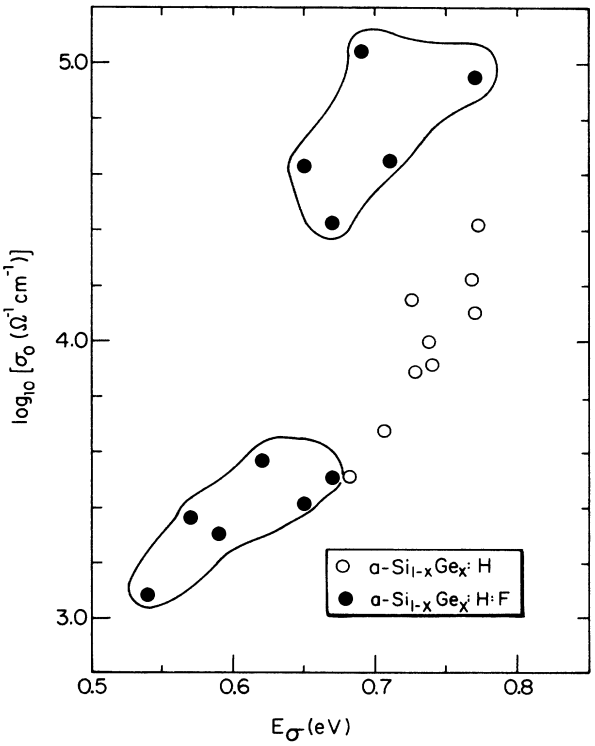

FIG. 7. Pre-exponential factor σ_0 for electrical conduction versus thermal activation energy E_σ.

Figure 8 shows the variation of $E_g/2-E_\sigma$ with x for the two types of material. For both types, the activation energies are within 100 meV of half of the gap. For the hydride-produced material, the Fermi level stays essentially at gap center. For the fluoride-produced films, the Fermi level usually lies above the center of the gap and there is more scatter in its position.

In order to extend our knowledge of the relative gap densities of states in hydride- and fluoride-derived alloys we have carried out space-charge-limited-current measurements[18] for samples with $x \approx 0.5$ and have compared them with those for a-Si:H. Whereas the latter samples had a density of states just above the Fermi level of 10^{16} $cm^{-3}eV^{-1}$, the density for a-$Si_{0.5}Ge_{0.5}$:H and a-$Si_{0.5}Ge_{0.5}$:H:F was about 10^{17} $cm^{-3}eV^{-1}$. All of the samples were measured in a sandwich geometry and the results found to be repeatable on samples from different runs.

Finally, the dangling-bond densities have been determined by electron spin resonance in samples with $x \approx 0.5$ produced from both hydrides and fluorides.[19] The first results for samples of a-$Si_{0.5}Ge_{0.5}$:H gave a Ge dangling-bond density of 6×10^{17} cm^{-3} and a Si dangling-bond density of 2×10^{16} cm^{-3}. For three sets of a-$Si_{1-x}Ge_x$:H:F samples, where the x value varied from 0.20 to 0.47, a Si dangling-bond density between 5×10^{16} and 10^{17} cm^{-3} was found but, surprisingly, no signal at the g value of the spin resonance from electrons on Ge dangling bonds. This intriguing result is being followed up (see Sec. VIII), but we note here simply that there is no evidence from the current measurements of a drastic reduction in the total dangling-bond density when the alloys are made from mixtures of fluorides.

VI. VARIATION WITH x OF THE PHOTORESPONSE OF a-$Si_{1-x}Ge_x$:H AND a-$Si_{1-x}Ge_x$:H:F

Figure 9 presents the results for the (quantum efficiency)(mobility)(lifetime) product, or $\eta\mu\tau$, deduced from our measurements of photoconductivity at room temperature on annealed (Staebler-Wronski A state)[29] samples illuminated by a flux of 10^{15} photons/cm^2 s of 1.96-eV radiation. Included are the x-dependent $\eta\mu\tau$ of our earlier study,[2] our measurements on a-$Si_{1-x}Ge_x$:H:F, and data from the Shimizu group.[32] All values of $\eta\mu\tau$ are corrected to take account of the penetration depth of the light. The crucial point made in this figure is that the $\eta\mu\tau$ product is almost always larger, sometimes by an order of magnitude, in the fluoride-derived samples of roughly 50-50 composition. These results suggest that an improved photoresponse from a-Si-Ge can be achieved by preparation from fluoride-sources gases. Two important points must be made and considered. The magnitude of the $\eta\mu\tau$ product can be very sensitive to the position of the Fermi level. Recognizing this fact, we have shown in Fig. 8(a) the variation in Fermi level, depicted as a departure of E_F from the center of the gap, for both hydride- and fluoride-produced samples, and in Fig. 8(b) the variation of $\eta\mu\tau$ for an expanded set of fluoride-produced samples as a function of their Fermi-level position. It is evident that there is no correlation between the magnitude of $\eta\mu\tau$ and the Fermi-level position for the fluoride-

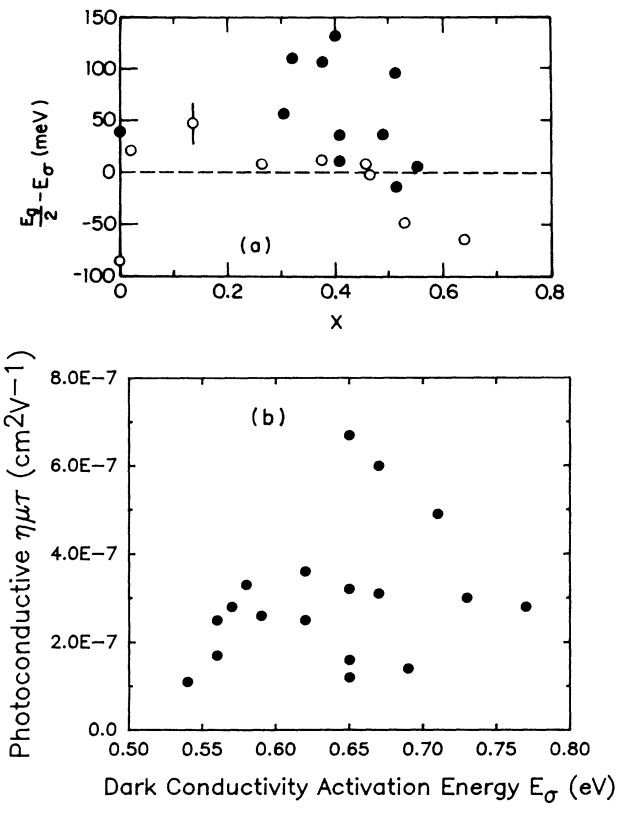

FIG. 8. (a) Variation of $E_g/2-E_\sigma$ with x. Open symbols refer to hydrides. Solid symbols refer to fluorides. (b) Variation of $\eta\mu\tau$ with dark-conductivity activation energy E_σ for a series of a-$Si_{1-x}Ge_x$:H:F alloys with band gap near 1.4 eV.

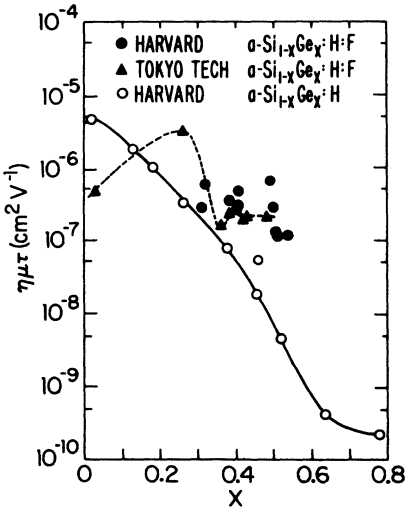

FIG. 9. Photoconductivity $\eta\mu\tau$ products vs x for hydride- and fluoride-derived alloys, measured at a photon energy of 1.96 eV.

produced samples. The second point concerns the photoconductivity experiment itself. All the measurements in this work were performed using (Cr) contacts in a coplanar geometry and 1.96-eV radiation which penetrates only a small fraction ($\sim 0.1-0.2$ μm) of the total thickness (2–4 μm) of the higher Ge content samples. This suggests the possibility that the "improved" photoresponse may be associated with some surface-related phenomena, e.g., surface band bending, contact effect or surface states rather than an overall improvement in the bulk properties. (For a recent discussion of this problem related to *a*-Si:H and *a*-Ge:H, see Ref. 33.) To test for surface-related effects, two further experiments have been conducted.[10–12] The first experiment involved the remeasurement of the steady-state photoconductivity in the coplanar electrode configuration using penetrating (1.5 eV) radiation to probe the bulk. The $\eta\mu\tau$ from steady-state photoconductivity is derived from

$$I = |e| F_0 l A(\eta\mu\tau) V/d \ ,$$

where I is the photocurrent for an applied voltage V, d is the separation of the coplanar contacts and l their length, A is the absorptance $(1-\mathcal{T})$, with $\mathcal{T}$ the transmittance, and F_0 is the density of photons/cm^2 s entering the sample. Empirically, I varies as $(F_0\alpha)^\gamma$ where α is the absorption coefficient, which implies that $\eta\mu\tau \propto (F_0\alpha)^{\gamma-1}$. We have chosen arbitrarily to refer all $(\eta\mu\tau)$ determinations to $(F_0\alpha)=10^{19}$ photons/cm^3 s at a photon energy of 1.5 eV, and so put

$$(\eta\mu\tau)^{1.5}_{10^{19}} = (\eta\mu\tau)^{1.5}_{\text{meas}} \left[\frac{(\alpha F)^{1.5}_{\text{meas}}}{10^{19}} \right]^{1-\gamma} .$$

This permits comparison of $(\eta\mu\tau)$ under the same conditions of created carrier density, thus making a first-order correction for the statistics of trapping and recombination. The explicit flux dependence of $(\eta\mu\tau)$ at any photon energy has also been experimentally confirmed. The second experiment, transient photoconductivity by the TOF method, was used as an alternative technique to determine $\mu\tau$ for electrons in the bulk, where possible on samples codeposited with the steady-state photoconductivity specimens. For the TOF experiments,[16] 2–5-μm-thick sandwich structures were produced consisting of 100 nm of Cr on Corning 7059 glass, the alloy, and a 10–20-nm, 3-mm-diameter, semitransparent top Cr Schottky contact. In this experiment, a weak 8-ns pulse of 3.68-eV radiation from a nitrogen laser creates an electron-hole density of approximately 10^{15} cm^{-3} to a depth of about 100 nm in the samples beneath the semitransparent electrode. A reverse bias electric field pulse (~ 7 ms) E is applied to the top contact about 20 to 200 μs before the laser pulse, i.e., in a time interval much less than the samples' dielectric relaxation time. This field extracts the electrons through the sample to the opposite (collecting) contact and the resulting phototransient $I(t)$ is recorded with a digitizer interfaced to a computer. The repetition rate of the laser is about 1 Hz. The integrated collected charge Q $[=\int I(t)dt]$ is determined as a function of the applied field E. The electron $\mu\tau$ product may be found by fitting the Q-versus-E plot to the Hecht[34] relation when all the electrons are collected, i.e., for low Ge contents, $x \lesssim 0.26$. For larger Ge contents, severe carrier loss prevents complete charge collection even at large E, and only the initial (low E) part is used. Decrease in the dielectric relaxation time with increasing conductivity and x value necessarily limits our $\mu\tau$ determination to x values of 0.4 or smaller. As for the steady-state experiments, the TOF measurements were taken in the Staebler-Wronski A state.[29]

Figure 10 summarizes the results from the two experiments. The x dependence of $\eta\mu\tau$ for the fluoride- and hydride-derived material is similar to that shown in Fig. 9, with the fluoride-derived material still possessing a superior photoresponse in the region $x \approx 0.5$. Thus surface-related effects in this x range are negligible. Independent confirmation of this result is suggested from analysis of TOF data[16] which indicate that while the depletion layer widths are about 1 μm for $x \approx 0$, they decrease rapidly down to about 0.1 μm at $x \approx 0.4$, with surface band bending of a few hundredths of an eV. The $\mu\tau$ products from TOF are about two orders of magnitude lower than the $(\eta\mu\tau)$'s deduced from steady-state photoconductivity, in the range of overlap $0.25 < x < 0.35$. This apparent discrepancy will be taken up in Sec. VIII. For *a*-$Si_{1-x}Ge_x$:H, the $\mu\tau$ products from TOF show a similar monotonic decrease with increasing x to that reported recently by Karg *et al.*[35] and Street *et al.*[28] Also, the behavior of $\mu\tau$ with x parallels that of $\eta\mu\tau$. The admittedly sparse data for $\mu\tau$ by TOF for *a*-$Si_{1-x}Ge_x$:H:F are comparable in magnitude to those for *a*-$Si_{1-x}Ge_x$:H.

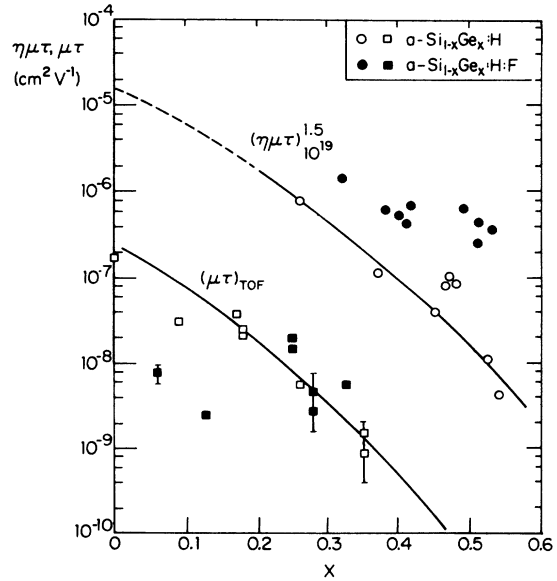

FIG. 10. Variation of normalized $\eta\mu\tau$ product from photoconductivity and $\mu\tau$ product from time of flight with x. The photoconductivity measurements were made with photons of energy 1.5 eV.

VII. VARIATION WITH x OF THE STRUCTURAL PROPERTIES OF a-$Si_{1-x}Ge_x$:H AND a-$Si_{1-x}Ge_x$:H:F

In this section, we report an extension of our earlier studies of infrared vibrational absorption and transmission electron microscopy[36] in a-$Si_{1-x}Ge_x$:H to similar studies on a-$Si_{1-x}Ge_x$:H:F. Figure 11, drawn from our earlier paper,[2] shows the principal H-related features of the spectrum: stretch modes of Si-H at 2090 cm^{-1} and 2000 cm^{-1}, and of Ge-H at 1975 cm^{-1} and 1875 cm^{-1}; bending modes in the region of 800–900 cm^{-1}; and a broad wagging vibration of Si-H and Ge-H centered on 630 cm^{-1}. With increasing T_s, the 2000-cm^{-1} Si-H mode and the 1875-cm^{-1} Ge-H mode dominate the stretch-mode spectrum and the bending modes disappear. In all of the spectra the Si-H modes dominate those of Ge-H in a ratio of approximately 8:1. A fuller description of these absorptions and their interpretation has already been given and will be discussed in Sec. VIII.

Figure 12 shows for comparison the infrared spectra of a-$Si_{0.5}Ge_{0.5}$:H:F and a-$Si_{0.5}Ge_{0.5}$:D:F prepared at $T_s = 300$ °C. The displacement of the H-related features at 2000, 1875, and 630 cm^{-1} to approximately $1/\sqrt{2}$ of these frequencies on replacing H with D is evident. It is clear that there are no *major* absorption frequencies to be associated with F, but that *minor* features near 1240 and 1100 cm^{-1} may be so connected. Figure 13 shows a Fourier-transform infrared (FTIR) transmission spectrum of an a-$Si_{0.5}Ge_{0.5}$:D:F sample between 400 and 1400 cm^{-1}. The peaks in absorption are superimposed on a spectrum showing interference fringes. The dip at 1350 cm^{-1} is assignable to Ge-D, that at 630 cm^{-1} to a bending mode of Si-D_2, and that near 1240 cm^{-1} is easily shown to be caused by an absorption in the Si substrate which is not quite balanced in a reference substrate. The dip at 1085 cm^{-1} is mysterious, but the frequency does not match any of the stretch modes suggested for SiF_n in the literature, the highest of which are 1010–1015 cm^{-1} [SiF_4, SiF_3, $(SiF_2)_n$].[37] The small dip near 824 cm^{-1} is not identified, but lands in the range suggested for SiF_2 bending modes. We conclude that the latter mode may be F connected, but that any absorption produced by F is inconsequential compared to those associated with H or D. This conclusion fits, of course, with the result of our electron microprobe examination that the concentration of F in our films is of the order of, or less than, 1 at. %. Analysis of the spectra of Fig. 12 shows that the preference ratio for attachment of H to Si rather than to Ge in a 50:50 alloy remains the same in the fluoride-derived films as it was in those made from a mixture of hydrides.

In our earlier work, we reported that a-$Si_{0.5}Ge_{0.5}$:H prepared at low temperature (230 °C), where the 2090-cm^{-1} stretch mode dominated that at 2000 cm^{-1}, showed clear evidence of an uptake of O as a function of time (1 at. % after 10 days). Samples of a-$Si_{0.5}Ge_{0.5}$:H prepared at 300 °C also showed clear evidence of O pick-up with time, although much less than for those prepared at 230 °C, while no O contamination and no O uptake with time was found for samples of a-$Si_{0.5}Ge_{0.5}$:H:F prepared at substrate temperatures between 200 and 350 °C.

Figure 14 compares the Raman spectra[38] of a-

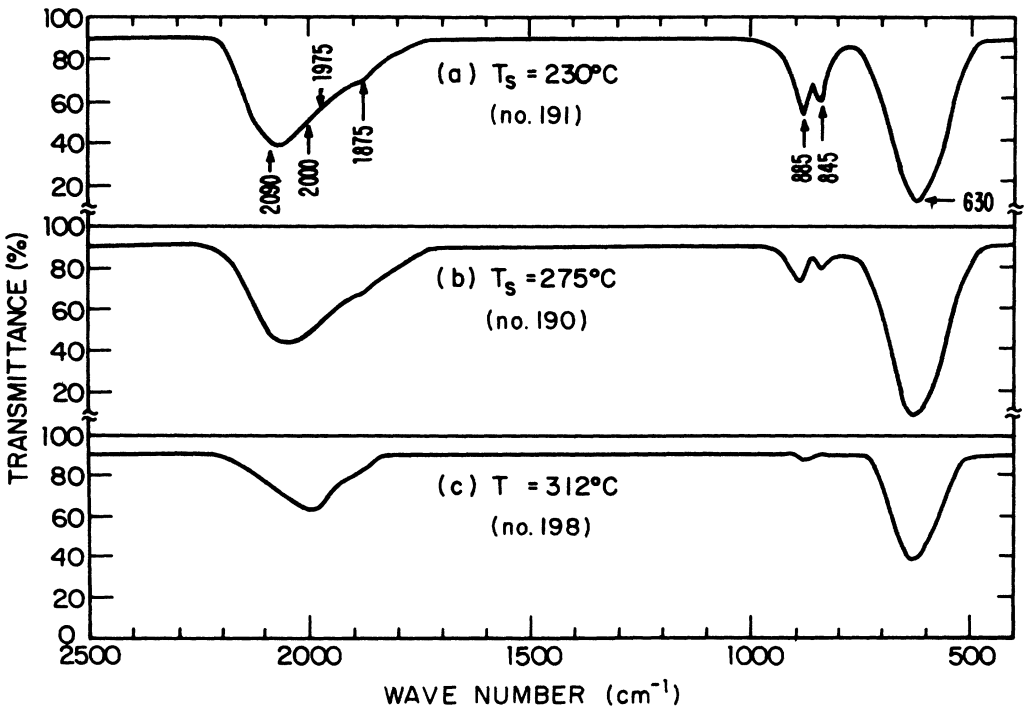

FIG. 11. Infrared absorption spectra of a-$Si_{0.5}Ge_{0.5}$:H prepared at (a) $T_s = 230$ °C, (b) 275 °C, and (c) 312 °C. The main features are labeled in (a). The numbers in parentheses identify the samples (after Ref. 2).

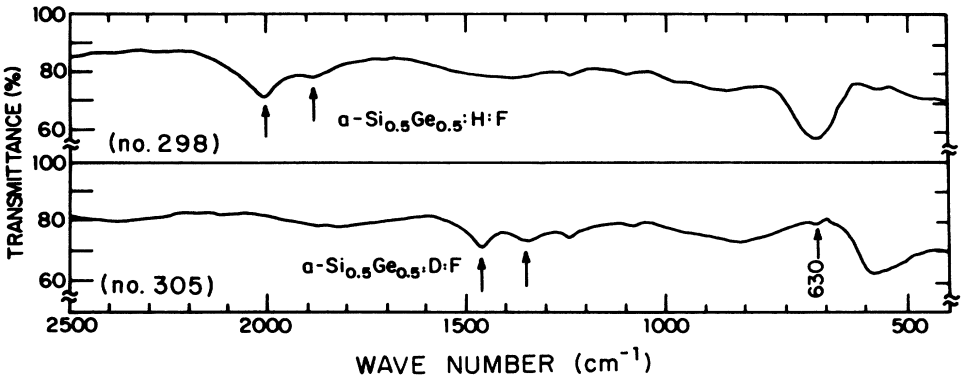

FIG. 12. Infrared absorption spectra of a-$Si_{0.5}Ge_{0.5}$:H:F and a-$Si_{0.5}Ge_{0.5}$:D:F alloys.

$Si_{0.5}Ge_{0.5}$:H and a-$Si_{0.5}Ge_{0.5}$:H:F. These spectra were taken, with a resolution of 3.9 cm^{-1}, on films approximately 50 nm thick co-deposited with the samples used for the transmission-electron-microscopy studies. The increase in counts below ~ 150 cm^{-1} is caused by stray light, and is greater for the fluoride-produced sample because it has a slightly rougher surface. The three peaks near 270, 370, and 470 cm^{-1} are assigned respectively to Ge-Ge, Ge-Si, and Si-Si optical mode vibrations.[39] There is some indication of a small peak near 200 cm^{-1} which we assign to a Si-Si acoustic mode. The peaks have the same positions and widths in the two preparations of sample, indicating that there are no major differences in the short-range order. Moreover, the areas under the three peaks have about the same ratios, indicating that the relative numbers of Ge-Ge, Ge-Si and Si-Si bonds are the same. Finally, there is no evidence of a mode attributable to F_2 near 890 cm^{-1}. Figure 15 shows the Raman spectrum of an a-SiGe:H:F film grown under conditions of low power such that the composition was over 99 at. % of Ge. The figure shows a clear crystalline Ge peak at 300 cm^{-1}.[40] This indicates the sensitivity of the Raman spectrum to small volumes of crystallinity and verifies that spectra such as those of Fig. 14 correspond to fully amorphous material.

Figure 16 shows TEM micrographs of approximately 50-nm-thick a-Si:H, a-Ge:H, and a-$Si_{0.5}Ge_{0.5}$:H films all prepared near 230 °C. The micrograph of a-Si:H shows weakly discernible microstructure; bulk films made under similar preparation conditions exhibit good photoelec-

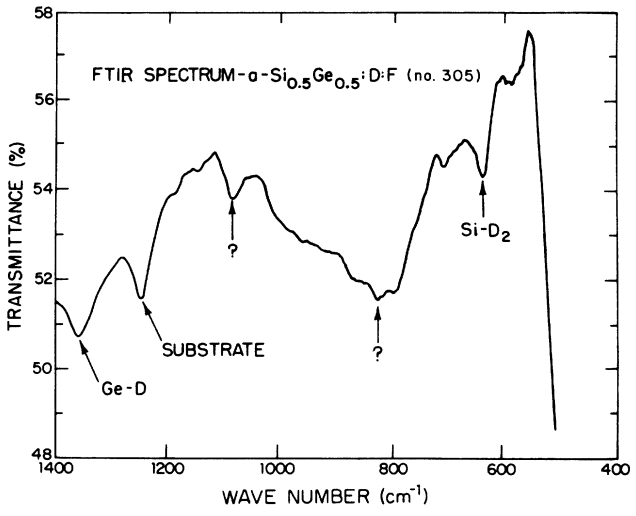

FIG. 13. FTIR transmission spectrum of a-$Si_{0.5}Ge_{0.5}$:D:F.

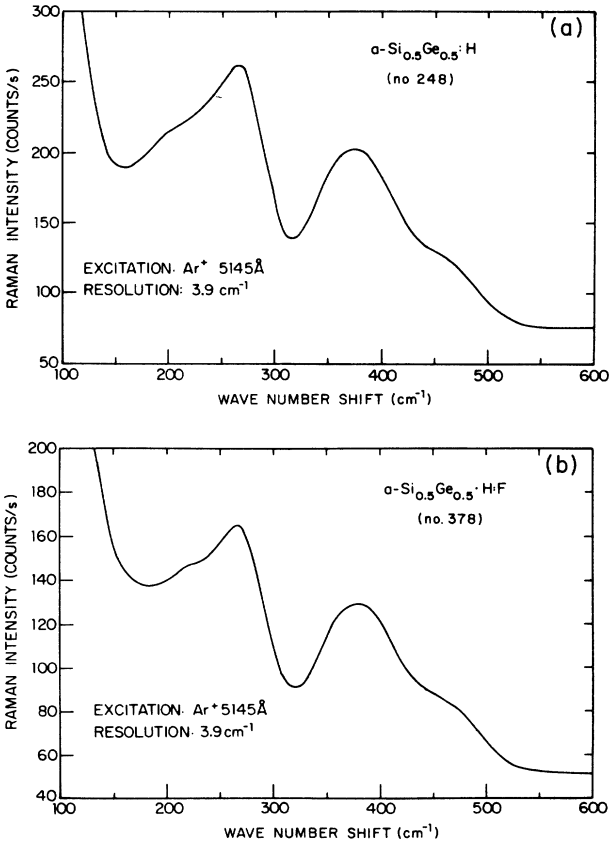

FIG. 14. Raman spectra of (a) a-$Si_{0.5}Ge_{0.5}$:H and (b) a-$Si_{0.5}Ge_{0.5}$:H:F.

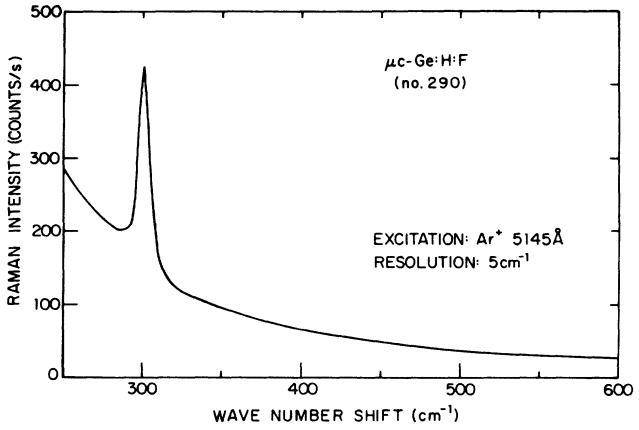

FIG. 15. Raman spectrum of a microcrystalline sample produced from fluorides.

tronic properties. In contrast, *a*-Ge:H shows distinct two-phase microstructure consisting of noncoalescing island regions (10–20 nm) of high electron density (dark regions) surrounded by lower-density tissue material. The *a*-$Si_{0.5}Ge_{0.5}$:H possesses a similar form of island-tissue structure. The bulk forms of both these materials show clear evidence of O uptake *and* poorer photoelectronic properties than unalloyed *a*-Si:H. As discussed in a previous publication,[2] structural inhomogeneity increases and the photoresponse deteriorates when the substrate temperature is decreased below the optimum value of 300 °C. In this paper we focus attention on Fig. 17, which compares TEM micrographs of *a*-$Si_{0.5}Ge_{0.5}$:H and *a*-$Si_{0.5}Ge_{0.5}$:H:F films, codeposited with films whose (identical) Raman spectra were shown in Fig. 14 and which were prepared at a T_s of 300 °C to have identical thicknesses of about 50 nm. It is evident that the microstructures are very different. Both show a two-phase structure on a similar scale. However, the fluoride-derived material shows much stronger contrast between the two phases and the boundaries are very different (more angular) in shape suggesting a quite different growth mechanism. Amorphicity of these specimens along with all other TEM specimens was confirmed by electron diffraction measurements. An attempt was made to probe the chemical composition on the 100-Å scale using x-ray microanalysis in a scanning transmission microscope. Problems associated with beam broadening through the films made this impossible.

VIII. DISCUSSION

Our discussion will be directed at two problems: first, the reason for the deterioration of the photoelectronic properties of amorphous silicon-germanium alloys compared to unalloyed silicon, and second, the reason for the improved photoconductivity of alloys produced from fluorides compared to those produced from hydrides.

Four solutions have been proposed for the first of these problems,[2] viz., (1) preferential attachment of H to Si dangling bonds, leaving many Ge-related defects and gap states in the alloys; (2) valence- and conduction-band tails

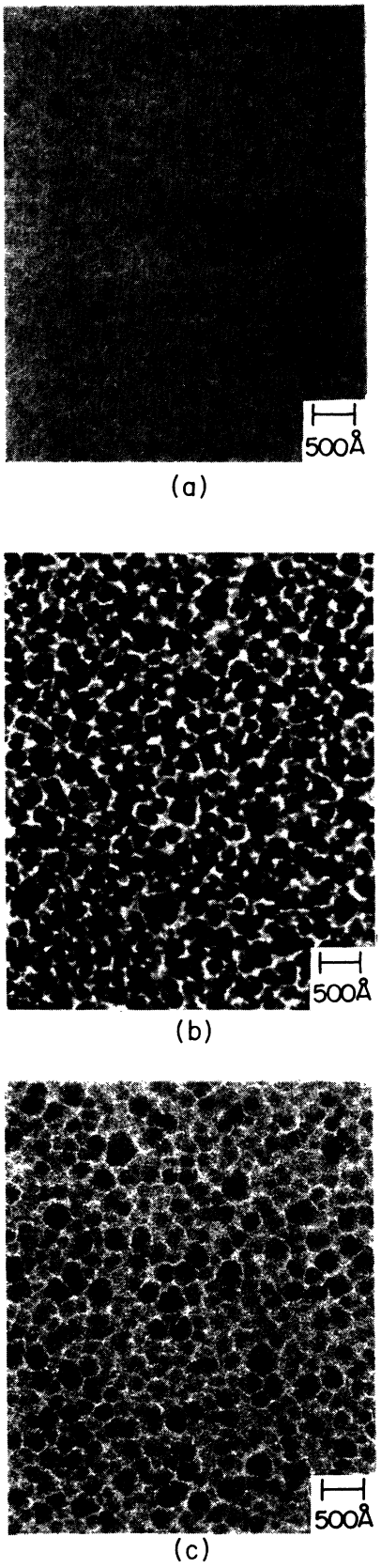

FIG. 16. Bright-field TEM images of (a) *a*-Si:H, (b) *a*-Ge:H, and (c) *a*-$Si_{0.5}Ge_{0.5}$:H. The specimens were prepared at substrate temperatures near 230 °C and are about 50 nm thick.

of states which are at least as broad as in a-Si:H, which implies a larger density of states near the middle of the energy gap in the narrower-gap material; (3) different gap density-of-states distribution in the alloys, involving both Si and Ge dangling-bond states at different energies so that, for most positions of the Fermi level, there are charged defects which easily trap carriers; and (4) increased heterostructure in the alloys, i.e., increased differences in island-tissue composition and properties, which affect phototransport.

In discussing these proposed solutions, we shall at first set aside the discrepancy in the $\mu\tau$ products estimated from photoconductivity and time-of-flight measurements displayed in Fig. 10, since the deterioration in $\mu\tau$ on adding Ge to the Si is present for both experiments.

The first solution has already been argued[41] to be inadequate since the magnitudes of the photoconductivity and photoluminescence are actually larger than would be expected if the Ge dangling bonds were as little "hydrogenated" as the infrared vibrational absorption would suggest. Dual magnetron sputtering[42] has been applied to equalize the H attachment to Si and Ge, but this does not appear to be the panacea for radical improvement of the properties. Our finding that the ratio of H attachments is the same in hydride- and fluoride-derived material, while the photoconductivity is much improved in the latter, also argues against the preferential attachment of H to Si as the root cause of problems with the alloys.

In order to consider the second and third possible reasons for deteriorated properties in the alloys, we show in Fig. 18 our proposed band structure[2] for a-$Si_{0.5}Ge_{0.5}$:H which is based on the following data and assumptions: (a) the decrease in $N(E)$ above the valence-band edge is given by the slope of the Urbach tail, i.e., by the magnitude of the E_0 of Fig. 3; (b) the decrease in $N(E)$ below the conduction-band edge is deduced from the time-dispersive transport of electrons in a-Si:H;[43] (c) the dangling-bond bands D^0 and D^- have the same FWHM, 0.2 eV, the maximum of the Ge D^0 band is at midgap in a-Ge:H,[44] the maximum of the Si D^0 band is roughly 1.0 eV below the conduction band in a-Si:H,[45] and the Ge and Si dangling-bond correlation energies are 0.1 (Ref. 44) and 0.35 eV,[46] respectively; (d) there may be, and probably are, so far unidentified defect states with energies below midgap. Models differing in some of the details have also been published, particularly in the relative ordering of the Ge and Si dangling-bond levels.[47]

It is evident from Fig. 4 that the decrease in $N(E)$ above the *valence-band* edge is slower in the alloys than in a-Si:H. Our TOF measurements[16] and those so far published imply that the *conduction-band* tail of a-

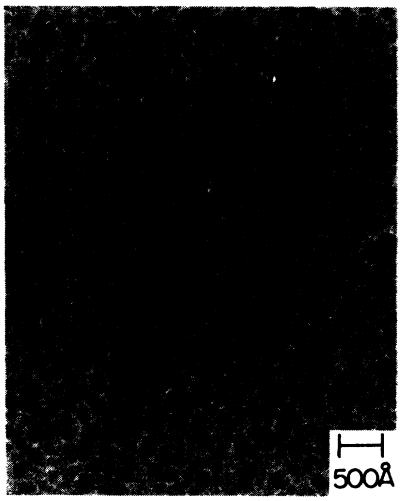

FIG. 17. Comparison of bright-field TEM images of (a) a-$Si_{0.5}Ge_{0.5}$:H, and (b) a-$Si_{0.5}Ge_{0.5}$:H:F. The specimens were prepared at 300 °C and are about 50 nm thick.

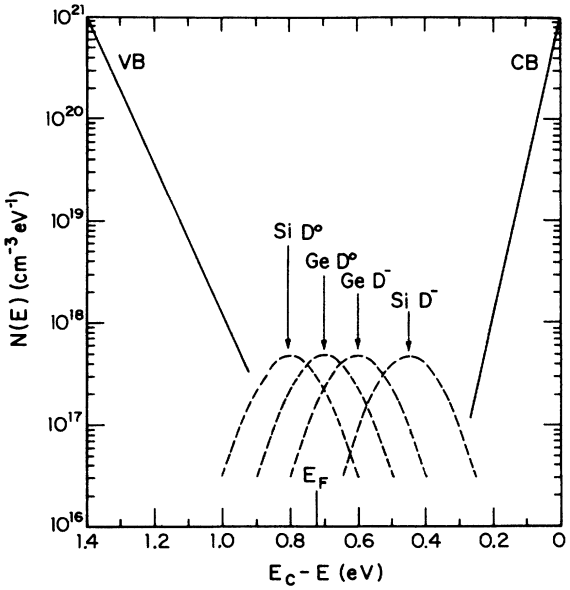

FIG. 18. Schematic band structure for a-$Si_{0.5}Ge_{0.5}$:H showing the energy of Si and Ge D^0 and D^- dangling bonds with respect to the conduction and valence bands, CB and VB (after Ref. 2).

$Si_{1-x}Ge_x$:H broadens slightly with increasing Ge content. Unfortunately, information on the conduction band tail is limited to alloys of low x ($x<0.35$) due to severe carrier loss and problems associated with dielectric relaxation at higher x. The evidence from our experiments for the broadening of the tail comes from the observation of a reduction in the electron drift mobility and an increase in the mobility thermal activation energy E_μ with increasing x; thus, for $x=0$, $\mu\sim 1$ $cm^2 s^{-1} V^{-1}$ and $E_\mu=0.11$ eV, while for $x=0.18$, $\mu\sim 0.3$ $cm^2 s^{-1} V^{-1}$, and $E_\mu=0.17$ eV (both mobilities measured with the same applied field of 10^4 $V cm^{-1}$). Similar results have been reported elsewhere.[28,35] The actual slope of the (exponential) tail has also been determined from TOF data. For instance, Weller *et al.*[14] find that the slope changes from 35 meV in *a*-Si:H to 60 meV in 1.45-eV band-gap alloy. Vanderhaghen and Longeaud[48] deduced a slope of 41 meV for an alloy of x value of 0.18. Karg *et al.*[35] obtain slopes of 22, 26, and 30 meV for x values of 0, 0.15, and 0.25, respectively. Consideration of these new data and details of band structure in Fig. 18 suggest that broadening of the conduction-band tail (and of the valence-band tail), howsoever caused, will contribute to the deterioration of the photoresponse. However, it is clear from Fig. 18 that the density of states near midgap is unlikely to be determined predominantly by the tail states. It therefore seems unlikely that altered tail state distributions are the sole cause of the deterioration in the alloy photoelectronic properties.

The third proposed reason for deterioration of the photoresponse of the alloys has two aspects to it: first, the probability that the total of defects may increase on alloying, and second, the probability that even for a fixed total of dangling bond and other defects, their wider distribution in energy will lead to the existence of charged traps. Both of these aspects seem to eventuate. The dangling bond density from ESR,[49,50] the sub-band-gap absorption from photoconductivity spectra, the density of states below the conduction-band edge as inferred from the drift mobility and dispersion parameters for electrons by TOF (see above), and the defect density to which the PL intensity is inversely proportional,[51] all increase with x. For $x\approx 0.5$, the gap density of states (GDOS) appears to be about an order of magnitude larger in the alloys, explaining the deterioration in their properties, without, of course, providing the basic reason for the state density increase.

The fourth proposed solution would appear to provide adequate reason for the larger GDOS.[52] The new results on the fluoride-derived materials support this model. Thus, contributions (2), (3), and (4) provide adequate reasons why the photoresponse in the alloys is poorer than in unalloyed *a*-Si:H. We now return to discuss the problem of the very different $\mu\tau$'s estimated, even for $x=0$, from the photoconductivity and TOF measurements shown in Fig. 10. This difference has been found before, but is seldom discussed.[53] In fact, a difference is not unexpected. First, the measuring conditions, particularly the photon flux and sample configuration in the two experiments, are very different. In the TOF technique, the total density of photoexcited electrons in one experiment is given by the product of the density in one optical pulse ($\sim 10^{15}$ cm^{-3} over a depth of about 100 nm) multiplied by the number of pulses (about 100). This averages to about 2.5×10^{15} cm^{-3} for a 4-μm-thick sample. By contrast, in the photoconductivity experiment, we illuminate with a steady-state photon flux of 10^{15} $cm^{-2} s^{-1}$, and other experimenters use densities (AM1) (air mass 1 or AM1) about a factor of 300 higher. Thus the photocarrier densities involved, the resultant carrier distribution in gap states, and the trapping lifetimes, are likely to be very different. Indeed, as we discussed in Sec. VI, the $\eta\mu\tau$ product is explicitly dependent on the photon flux or more specifically on the carrier generation rate. Another important difference is in the configuration of the experiment: The TOF experiment is carried out in a sandwich configuration, while the photoconductivity experiment involves transport between two coplanar electrodes. Thus the latter experiment is much more susceptible to surface states and surface band bending.[33] However, from Fig. 10 (normalized $\eta\mu\tau$ measured using penetrating radiation) and depletion layer width, surface-band-bending calculations from TOF data, we see that surface effects are negligible, at least for the Ge contents investigated ($x>0.25$). Even if the TOF and steady-state photoconductivity experiments were performed with the same photocreated carrier densities, a difference in $\mu\tau$ would *still* be observed; the important factor is time scale. If the mobility μ is taken to be the mobility in the extended states of the conduction band, then the τ in the TOF experiment is the integrated time in the band before the first deep trapping event. Since the TOF measurement lasts of the order of 10 μs, release from a deep trap (as distinct from release from a shallow band-tail trap) does not occur on the time scale of the experiment. In the steady-state experiment, on the other hand, trapping is followed by release until the carrier ultimately recombines with a hole. It is well known that this can be a lengthy process and many experiments have been done to demonstrate the release of such trapped carriers.[54]

It may be concluded from the above that both the TOF and steady-state photoconductivity experiments confirm a deterioration in $\mu\tau$ with alloying and that the apparent discrepancy in the magnitude of the $\mu\tau$ reflects the (very) different trapping statistics involved in the two experiments.

We now direct our attention to the second problem, that of the reason for the improved photoresponse of fluoride-derived alloys. Our experimental results demonstrate that any changes in gap density-of-states structure between the hydride- and fluoride-derived materials are subtle.

First, as already noted, the sub-band-gap absorption and PL intensity, which are presumably measures of the relative gap density of states,[55] do not change significantly or consistently in the hydride and fluoride materials. In fact, we usually find an increased sub-band-gap absorption in our fluoride-derived material, whereas Guha[3] reports the opposite; in any event, the magnitude of the change is insufficient to account for the change in $\eta\mu\tau$.

We consider next our space-charge-limited current (SCLC) results, which must be presented with carefully described caveats. Our preliminary SCLC measurements[18] on n^+-i-n^+ structures of a-$Si_{0.5}Ge_{0.5}$:H and a-$Si_{0.5}Ge_{0.5}$:H:F indicate densities of states just above the Fermi level which are both about an order of magnitude larger than in a-Si:H. However, the activation energies for transport across these sandwich structures are different, and suggest a Fermi level about 0.2 eV closer to the conduction-band edge in the material produced from fluorides. Thus, there remains the possibility that the densities of states at the same energetic position in the band gap are different in the two preparations. We expect that the conductivity activation energies, 0.6 eV for the a-$Si_{0.5}Ge_{0.5}$:H sandwiches and 0.4 eV for the a-$Si_{0.5}Ge_{0.5}$:H:F ones, are reduced from the values we usually find (0.72 ± 0.01 and 0.63 ± 0.06 eV, respectively) for intrinsic layers of this composition, by P doping after the n^+ deposition in our single-chamber system. If so, it is interesting that the Fermi-level displacement is consistently different between the three unfluorinated and two fluorinated samples examined. A greater incorporation of P in the fluorinated sample, or a smaller gap DOS to be compensated in the fluorinated sample, or a change in the ratio of P incorporated in fourfold (doping) or threefold (nondoping but potentially defect-creating) configurations, are all possible explanations for the observations. In addition to these uncertainties, it must be remembered that a consistently higher Fermi level will lead to improved electron photoconductivity, which will be discussed below. One relief from these difficulties would be to make the n^+-i-n^+ structures in a multiple-chamber system. Another is to study SCLC in a coplanar configuration. We have attempted such measurements, but have encountered two difficulties. The first is that the current-voltage relationship did not follow the expected scaling law when the distance between the contacts was varied, and the second was an unacceptable irreproducibility in the measured current-voltage characteristic. One possible reason for these problems is the occurrence of surface conductivity. In any event, more study needs to be done before these data can be interpreted with confidence. In summary, although the SCLC results appear to show about the same density of states in the two preparations of alloy, there do remain problems of interpretation connected with Fermi levels displaced by different amounts from the intrinsic material. Similar densities of states from SCLC measurements to those reported here have been obtained by Guha *et al.*[56]

The neutral dangling-bond density in our a-$Si_{0.5}Ge_{0.5}$:H films is similar to values reported elsewhere[49,50] for this Ge concentration and is about at least two orders of magnitude greater than the density found in high-quality undoped a-Si:H films.[57] However, no signal corresponding to the known g value for Ge dangling bonds was found by the Naval Research Laboratory (NRL) group[19] in the fluoride-derived set of alloys of four different x values. Interestingly, Shimizu and coworkers[58] found a low spin density, putting an upper limit of 7×10^{15} cm^{-3} for their a-$Si_{1-x}Ge_x$:H:F material which had an x value of 0.3. Also, preliminary results by Aljishi *et al.*[5] indicate neutral Ge dangling-bond densities in their fluoride-derived alloys which are at least an order of magnitude lower ($\sim10^{16}$ cm^{-3} cf. $\sim10^{17}$ cm^{-3}) than found for hydride-derived alloys. There are several possible explanations for a low or apparently absent ESR signal for Ge. The obvious one is that the density of dangling bonds is at or below the detection limit for the apparatus and the sample volume used, but this seems implausible, at least for our material, since the signal from Si dangling bonds (5×10^{16}–10^{17} cm^{-3}) is easily seen. A second possibility is that any Ge dangling bonds are either empty or doubly occupied. The latter circumstance is consistent with a displaced Fermi level which is highly probable since the results shown in Fig. 8 indicate that the Fermi level for the fluoride-derived material is usually slightly above midgap. A similar conclusion was reached by Aljishi *et al.*[5] Interpretation of the significance of the results for a-$Si_{1-x}Ge_x$:H:F in terms of density of states is therefore limited. More study is required.

The fourth route to a determination of the gap state densities is through $\mu\tau$ measurements by the TOF method. The assembly of measurements on hydride-derived material displayed in Fig. 10 is consistent with a monotonic decrease in electron $\mu\tau$. The variation in $\mu\tau$ product with x for the fluoride-derived material is less surely established, but it does appear that the $\mu\tau$'s for electrons are little different from those for hydride-produced samples. In order to separate out the changes in μ and τ, we have analyzed our current-versus-time photoconductivity transients to obtain the drift mobilities μ in the two types of preparation. The results indicate no significant differences in the drift mobilities for the same x and therefore, also, no differences in the deep trapping times. This fits the observations of parallel monotonic increases in trap state densities in both types of material.

In partial summary, our analysis of our measurements of sub-band-gap absorption, photoluminescence, space-charge-limited currents, electron spin resonance, and time-of-flight transport suggests that there are few significant differences in the gap densities of states in hydride- and fluoride-derived alloys. The explanation for the order-of-magnitude higher photoconductivity in the latter preparation must be sought elsewhere. Before doing so, we wish to mention and reject two other reasons for improvement in fluoride-derived alloys. The first of these is the possibility that a Fermi level consistently closer to the conduction-band edge in the bulk of the fluoride-derived material might explain the improved photoresponse. As was stated in Sec. VI we found no correlation between the magnitude of $\eta\mu\tau$ and the Fermi-level position for the fluoride-derived samples of band gap near 1.5 eV.

The second possible reason for improvement in the fluoride-derived material is the presence of F *in the alloy.* Our microprobe measurements suggest a concentration of F of the order of 1 at. %, and our infrared and Raman results confirm this small percentage. For comparison, Tsuda *et al.*[4] report less than 0.6%, S. Oda *et al.*[58] less than 1%, and the Energy Conversion Devices (ECD) group less than 1%.[59] The Princeton group[60] reports F concentrations of about 1 at. %. We conclude that the

presence of F *in the film,* replacing H, must be rejected as a major contributory factor to the improved photoresponse, in contradiction to the position advocated by Ovshinsky and Adler.[61] This was, indeed, anticipated by Weil *et al.*[62] who reported from studies on *a*-Si:F (no H present) that, while both H and F passivated dangling bonds, the H led to a relief of strain in the network while F did not. Weil *et al.* found that *a*-Si:F had rather poor photoelectronic properties.

Changes in the heterostructure have been consistently advocated by our group as a contributory reason for the deterioration in photoelectronic properties. The present results confirm that increased nonuniformity of the alloy films, on a scale of 10–50 nm, compared to unalloyed *a*-Si:H as evidenced by the TEM micrographs,[2] the changes in infrared absorption spectra,[2] and the low-temperature evolution of hydrogen in gas evolution studies,[63] occurs coincidentally with the observation of poorer photoelectronic properties. The present data also provide significant evidence for differences in the heterostructure of hydride- and fluoride-derived alloys, which we hypothesize is the fundamental reason for the differences in photoresponse of alloys with $x \approx 0.5$. We list next, in approximate order of significance, the evidence concerning these differences: (1) TEM micrographs, (2) deuteron quadrupole magnetic resonance measurements, (3) uptake of O as a function of time, and (4) photoluminescence peak linewidth.

The TEM micrographs indicate that there are major differences in the island-tissue structure in the two preparations of material. However, we have been unable to this point to determine with our microscope any local differences in chemical composition on a scale of 5–10 nm.

Deuteron quadrupole magnetic resonance measurements[13] have recently been carried out by the group of Professor R. Norberg at Washington University on samples prepared at Xerox Palo Alto Research Center and at Harvard University. We briefly summarize their findings here. DMR line shapes and relaxation times have distinguished five different localized hydrogen (deuterium) configurations, viz., (a) tightly bound D, (b) weakly bound D, (c) molecular D_2 "absorbed" on rough microvoid surfaces, (d) bulk molecular D_2 located well removed from microvoid surfaces, and (e) isolated molecular D_2 in poor "contact" with other D or D_2. The results depend on the deposition conditions, but, specifically, they show clear differences in void morphology between silicon-germanium alloys produced from hydrides and fluorides, as if the D_2 in the hydride material were isolated, while the D_2 in the fluoride were interacting, as in bulk D_2. Obviously this powerful technique needs to be developed further in order to make precise the inferences from it, but the conclusion of the existence of structural differences revealed by it should remain unaffected.

Our third item of evidence is the observation that films of *a*-$Si_{1-x}Ge_x$:H:F do not take up O as a function of time, as had been very clearly demonstrated for *a*-$Si_{1-x}Ge_x$:H.

Our information concerning the FWHM of the PL, although statistically significant, is hard to interpret in a very definite fashion. The narrower line widths for the *a*-$Si_{0.5}Ge_{0.5}$:H:F films would normally be interpreted as implying a less disordered structure. However, the slopes of the Urbach tails in the absorption spectra are the same, and the gap-state densities also. It is possible, though unlikely based on the TOF results, that the conduction-band tail is sharper in the fluoride-derived material. Aljishi *et al.* report that the tail is much broader in the fluoride-derived alloy than in *a*-Si:H.[64] This would rule out any influence of the microstructure on the FWHM.

It is possible to construct a simple model to explain the improved photoresponse achieved with the fluoride-derived alloys, based on the above evidence for a different two-phase microstructure and on the specific details of dark transport for the two alloy preparations. We recall from Fig. 7, which shows the pre-exponential factor σ_0 versus the thermal activation energy, E_σ, for dark conductivity, that the data for *a*-$Si_{1-x}Ge_x$:H were bunched together in one group sandwiched between the *a*-$Si_{1-x}Ge_x$:H:F data. From this, we may postulate a structural model, illustrated in Fig. 19, which permits two transport paths at different energies. Transport in the dark may proceed by either of the paths, which are not too different in conductance. Phototransport, which is not subject to equilibrium carrier statistics, is postulated to occur via the islands—the path of higher σ_0 and presumably higher μ. Consistent with this, *all* of the *a*-$Si_{1-x}Ge_x$:H:F samples of Fig. 9, with either low or high σ_0, give $\eta\mu\tau$ products in the same range. These $\eta\mu\tau$'s are as much as an order of magnitude larger than those for *a*-$Si_{1-x}Ge_x$:H, which show values lying between the high and low extremes for *a*-$Si_{1-x}Ge_x$:H:F. On the basis of this model, one might expect the $\mu\tau$ products from the TOF experiment, which essentially measures transport in the dark, to follow the σ_0 values. However, the data for the fluoride-derived samples are too sparse to test this prediction.

An alternative model for the improved photoresponse achieved with the *a*-$Si_{1-x}Ge_x$:H:F alloy is simply that the recombination lifetime (but not necessarily the first deep-trapping time) is larger. One might expect some

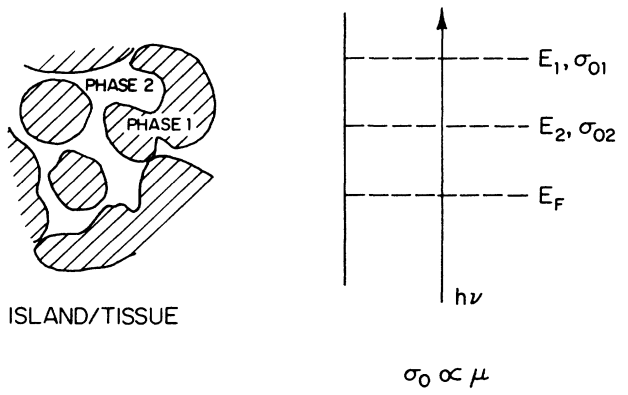

FIG. 19. Model for phototransport in fluoride-derived alloys.

evidence of this to show in one of the measurements to probe the gap DOS—which is not clear. An improved recombination lifetime may be linked speculatively to the different microstructure.

We note, in passing, that Slobodin *et al.*[65] have studied the properties of films prepared either from plasmas of (SiH_4+GeF_4) or ($SiF_4+GeF_4+H_2$). Although the ir spectra, sub-band-gap absorption spectra, dark-conduction activation energies, carrier drift mobilities, and deep-trapping lifetimes of the two preparations of alloy were very similar, the films made from the latter gas combination had an order-of-magnitude greater photoconductivity. These workers concluded that they agreed with our earlier deduction,[6] based on preliminary data, that altered microstructure was the cause, and speculated that the plasma of ($SiF_4+GeF_4+H_2$) might have fewer polymerization reactions and thus yield films with a closer microstructure.

IX. CONCLUSIONS

This work reinforces the conclusions of our earlier study[2] that both band-structure changes and an increased nonuniformity of microstructure are responsible for the deterioration in photoelectronic properties of Ge-rich alloys of a-$Si_{1-x}Ge_x$:H. It establishes also that there are significant differences in *microstructure* when the Si-Ge alloys are made from a mixture of SiF_4 and GeF_4 with H_2, rather than from a mixture of SiH_4 and GeH_4. This conclusion is based on the following facts, here summarized from the main text: (1) differences in TEM micrographs for films which have identical Raman spectra and for which similarly produced films have very different properties, (2) differences in deuteron nuclear quadrupole resonance, interpreted in terms of a different void structure, and (3) differences in post-deposition pick-up of O revealed by infrared absorption spectra, which imply differences in accessible paths into the film. These differences in microstructure are hypothesized to cause, or could be correlated with, differences in structure near the surface of the film, which result in very different photoconductivities. Facts suggesting that the structure and the related band structure in the *bulk of the film* are *not* responsible for the differences in photoresponse, on the other hand, include the following: (4) the Raman spectra are identical, (5) the absorption spectra from 0.8 to 2.0 eV are essentially the same, (6) the PL spectra are principally different only in the FWHM, and (7) the gap densities of states, measured by SCLC or ESR, are the same. Finally, local passivation of dangling bonds by F rather than H is not regarded as an important cause, since (8) only 1% of F is incorporated in any of the films. Finally, we note again[14] that silicon-germanium alloys with photoelectronic properties possibly as good as, or even superior to, those of the alloys made from fluorine-containing gases reported here, but which contain only hydrogen as bond compensator, have been reported from several laboratories. Unfortunately, in most instances the position of the Fermi level has not been reported and there is no discussion of microstructure.

ACKNOWLEDGMENTS

The authors wish to thank B. F. Bateman, Y. F. Chen, J. Hanna, C. Hayzelden, Y. L. He, S. J. Jones, P. B. Kirby, S. M. Lee, F. Moraes, W. A. Turner, and Z. L. Sun for their collaboration in our experimental program. We also acknowledge collaborations with S. Asher of the Solar Energy Research Institute (Golden, CO), W. E. Carlos and U. Strom of the U.S. Naval Research Laboratory (Washington, D.C.), and R. E. Norberg and co-workers at Washington University (St. Louis, MO), and discussions with E. A. Schiff of Syracuse University (Syracuse, NY). This work was funded in part by Contract No. XB-7-06071 with the Solar Energy Research Institute (SERI), in part by Grant No. DMR-86-14003 with the National Science Foundation (NSF), and in part by the Division of Applied Sciences of Harvard University.

---

*Present address: Amoco Research Center, P.O. Box 400, Naperville, IL 60566.

†Present address: Massachusetts Institute of Technology, P.O. Box 73, Lexington, MA 02173-0073.

[1]See, for instance, articles in *Semiconductors and Semimetals,* edited by R. K. Willardson and A. C. Beer (Academic, Orlando, 1984), Vol. 21 D.

[2]K. D. Mackenzie, J. R. Eggert, D. J. Leopold, Y. M. Li, S. Lin, and W. Paul, Phys. Rev. B **31**, 2198 (1985).

[3]S. Guha, J. Non-Cryst. Solids **77&78**, 1451 (1985).

[4]S. Tsuda, H. Tarui, H. Haku, Y. Nakashima, Y. Hishikawa, S. Nakano, and Y. Kuwano, J. Non-Cryst. Solids **77&78**, 845 (1985).

[5]S. Aljishi, Z. E. Smith, D. Slobodin, J. Kolodzey, V. Chu, R. Schwarz, and S. Wagner, in *Materials Research Society Symposia Proceedings,* edited by D. Adler, Y. Hamakawa, and A. Madan (Materials Research Society, Pittsburgh, 1986), Vol. 70, p. 269.

[6]K. D. Mackenzie, J. Hanna, J. R. Eggert, Y. M. Li, Z. L. Sun, and W. Paul, J. Non-Cryst. Solids **77&78**, 881 (1985).

[7]K. Nozawa, Y. Yamaguchi, J. Hanna, and I. Shimizu, J. Non-Cryst. Solids **59&60**, 533 (1983).

[8]A. Madan, S. R. Ovshinsky, and E. Benn, Philos. Mag. **40**, 259 (1978).

[9]W. Paul, in *Fundamental Physics of Amorphous Semiconductors,* Vol. 25 of *Springer Series in Solid State Sciences,* edited by F. Yonezawa (Springer, Heidelberg, 1981), p. 72.

[10]K. D. Mackenzie and W. Paul, in *Materials Research Society Symposia Proceedings,* edited by D. Adler, Y. Hamakawa, A. Madan, and M. Thompson (Materials Research Society, Pittsburgh, 1987), Vol. 95, p. 281.

[11]K. D. Mackenzie, J. H. Burnett, J. R. Eggert, Y. M. Li, and W. Paul, in Proceedings of the 12th International Conference on Amorphous and Liquid Semiconductors [J. Non-Cryst. Solids **97&98**, 1019 (1987)].

[12]K. D. Mackenzie and W. Paul, in Proceedings of the 12th International Conference on Amorphous and Liquid Semiconductors [J. Non-Cryst. Solids **97&98**, 1055 (1987)].

[13]V. P. Bork, P. A. Fedders, R. E. Norberg, D. J. Leopold, K. D. Mackenzie, and W. Paul, J. Non-Cryst. Solids **77&78**, 715 (1985); V. P. Bork, P. A. Fedders, R. E. Norberg, D. J. Leopold, K. D. Mackenzie, and W. Paul, in *Hydrogen in Disordered and Amorphous Solids,* edited by G. Bambakidis and R. C. Bowman, Jr. (Plenum, New York, 1986), p. 111; V. P. Bork, P. A. Fedders, R. E. Norberg, D. J. Leopold, K. D. Mackenzie, and W. Paul, in *Materials Research Society Symposia Proceedings,* edited by D. Adler, Y. Hamakawa, and A. Madan (Materials Research Society, Pittsburgh, 1986), Vol. 70, p. 307.

[14]By conventional (diode) rf glow discharge, triode rf glow discharge and photochemical vapor deposition techniques, higher quality a-$Si_{1-x}Ge_x$:H alloys have been produced. See, for instance, Ref. 4; H. Itozaki, N. Fujita, and H. Hitotsuyanagi, in *Materials Research Society Symposia Proceedings,* edited by D. Adler, A. Madan, and M. J. Thompson (Materials Research Society, Pittsburgh, 1985), Vol. 49, p. 161; B. von Roedern, A. H. Mahan, T. F. McMahon, and A. Madan, *ibid.*, p. 167; M. Konagai, H. Takei, T. Tanaka, W. K. Kim, A. Yamada, J. Kenne, S. Nishida, H. Tasaki, P. Sichanugrist, C. Katagiri, J. Takada, and K. Takahashi, in Solar Energy Research Institute Report No. SERI/CP2112654, 1985 (unpublished); A. Matsuda, M. Koyama, N. Ikuchi, Y. Imanishi, and K. Tanaka, Jpn. J. Appl. Phys. **25**, L54 (1986); S. Tsuda, H. Haku, H. Tarui, T. Matsuyama, K. Sayama, Y. Nakashima, S. Nakano, M. Ohnishi, and Y. Kuwano, in *Materials Research Society Symposia Proceedings,* edited by D. Adler, Y. Hamakawa, A. Madan, and M. Thompson (Materials Research Society, Pittsburgh, 1987), Vol. 95, p. 311; T. Watanabe, M. Tanaka, K. Azuma, M. Nakatani, T. Sonobe, and T. Shimida, Jpn. J. Appl. Phys. **26**, L288 (1987); H. C. Weller, S. M. Paasche, C. E. Nebel, and G. H. Bauer, in Proceedings of the 12th International Conference on Amorphous and Liquid Semiconductors [J. Non-Cryst. Solids **97&98**, 1071 (1987)].

[15]The SiF_4 and H_2 gases were supplied by Matheson and the GeF_4 gas supplied by Cerac.

[16]K. D. Mackenzie and W. Paul (unpublished).

[17]A description of the TOF apparatus is given by P. B. Kirby and W. Paul, Phys. Rev. B **29**, 826 (1984).

[18]Space-charge-limited-current measurements performed by Y. F. Chen and W. A. Turner. See R. L. Weisfield, J. Appl. Phys. **54**, 6401 (1983), for details on the analysis.

[19]Measurements carried out by Drs. W. E. Carlos and U. Strom of the Naval Research Laboratory, Washington, D.C. (unpublished).

[20]A technical description of the apparatus may be found in the SERI Technical Reports of February 1983 and October 1983 under SERI Subcontract No. XB-2-02144-1 (unpublished), and also in Ref. 2.

[21]SIMS analysis carried out by Dr. S. Asher of the Solar Energy Research Institute, Golden, CO (unpublished).

[22]Cameca MBX unit with Tracor Northern automation operated by David Lange of Harvard University.

[23]R. W. Collins, Ph.D. thesis, Harvard University, 1982; J. R. Eggert, Ph.D. thesis, Harvard University, 1986.

[24]H. G. Grimmeiss and L. A. Ledebo, J. Appl. Phys. **46**, 2155 (1975); M. Vanecek, J. Kocka, J. Stuchlik, Z. Kozisek, O. Sticka, and A. Triska, Sol. Energy Mater. **8**, 411 (1983); J. Kocka, J. Vanecek, A. Kozisek, O. Sticka, and J. Beichler, J. Non-Cryst. Solids **59&60**, 293 (1983).

[25]J. Tauc, R. Grigorovici, and A. Vancu, Phys. Status Solidi **15**, 627 (1966).

[26]As noted earlier, variations in x across the substrate platform in depositions from fluorides rendered an estimate of x for the PL samples more difficult than for the hydride-derived ones. Consequently, we used the value of E_{PL} versus x for the hydride-derived samples to estimate x for the fluoride materials. To check the validity of this procedure, we determined the actual Ge content of some of the fluoride-derived samples by electron microprobe analysis.

[27]M. Gal, J. M. Viner, P. C. Taylor, and R. D. Wieting, Phys. Rev. B **31**, 4060 (1985); R. Ranganathan, M. Gal, J. M. Viner, and P. C. Taylor, Phys. Rev. B **35**, 9222 (1987).

[28]R. A. Street, C. C. Tsai, M. Stutzmann, and J. Kakalios, Philos. Mag. **B56**, 289 (1987).

[29]D. L. Staebler and C. R. Wronski, Appl. Phys. Lett. **31**, 292 (1977).

[30]See D. A. Anderson and W. Paul, Philos. Mag. B **44**, 187 (1981), or W. Paul and D. A. Anderson, Sol. Energy Mater. **5**, 229 (1981) for illustration and earlier references.

[31]W. Meyer and H. Neldel, Z. Tech. Phys. **18**, 588 (1937).

[32]K. Nozawa, Master's thesis, Tokyo Institute of Technology, 1984.

[33]M. Tanelian, Philos. Mag. B **45**, 435 (1982); R. A. Street, M. J. Thompson, and N. M. Johnson, Philos. Mag. B **51**, 1 (1985); P. B. Kirby, D. W. MacLeod, and W. Paul, Philos. Mag. B **51**, 389 (1985); G. N. Parsons, C. Kusano, and G. Lucovsky, J. Vac. Sci. Technol. A **5**, 1655 (1987).

[34]K. Hecht, Z. Phys. **77**, 235 (1932).

[35]F. Karg, W. Kruhler, M. Moller, and K. von Klitzing, J. Appl. Phys. **60**, 2016 (1986).

[36]Investigation done in collaboration with Professor Clive Hayzelden of Harvard University on a Philips EM420T electron microscope (unpublished).

[37]See, for example, B. K. Agrawal, Phys. Rev. Lett. **46**, 774 (1981).

[38]The Raman spectra were taken with a SPEX double monochromator using a photomultiplier tube in the phonon counting mode. The excitation source was the Ar^+ 5145-Å line, focused with a cylindrical lens. Collection was done in the near backscattering geometry.

[39]J. S. Lannin, in *Semiconductors and Semimetals,* edited by R. K. Willardson and A. C. Beer (Academic, Orlando, 1984), Vol. 21 B, p. 159.

[40]D. S. Shen, J. Kolodzey, D. Slobodin, J. P. Conde, C. Lane, I. H. Campbell, P. M. Fauchet, and S. Wagner, in *Materials Research Society Symposia Proceedings,* edited by D. Adler, Y. Hamakawa, and A. Madan (Materials Research Society, Pittsburgh, 1986), Vol. 70, p. 301.

[41]B. von Roedern, D. K. Paul, J. Blake, R. W. Collins, G. Moddel, and W. Paul, Phys. Rev. B **25**, 7678 (1982).

[42]R. A. Rudder, J. W. Cook, Jr., and G. Lucovsky, Appl. Phys. Lett. **45**, 887 (1984); R. A. Rudder, G. N. Parsons, J. W. Cook, Jr., and G. Lucovsky, J. Non-Cryst. Solids **77&78**, 885 (1985).

[43]T. Tiedje, J. M. Cebulka, D. L. Morel, and B. Abeles, Phys. Rev. Lett. **46**, 1425 (1981).

[44]M. Stutzmann, J. Stuke, and H. Dersch, Phys. Status Solidi B **115**, 141 (1983).

[45]See discussion in Ref. 2 and also P. G. LeComber and W. E. Spear, Philos. Mag. B **53**, L1 (1986).

[46]See, for instance, H. Dersch, J. Stuke, and J. Beichler, Phys. Status Solidi B **105**, 265 (1981); W. B. Jackson, Solid State Commun. **44**, 477 (1982).

[47]M. Stutzmann, R. J. Nemanich, and J. Stuke, Phys. Rev. B **30**, 3595 (1984); A. Skumanich, A. Frova, and N. M. Amer, Solid

State Commun. **54**, 597 (1985); C. Y. Huang, S. Guha, and S. J. Hudgens, J. Non-Cryst. Solids **66**, 187 (1984); G. Lucovsky, J. W. Cook Jr., R. A. Rudder, and G. N. Parsons, in Solar Energy Research Institute Report No. SERI/CP2112654, 1985 (unpublished), and also Ref. 5.

[48]R. Vanderhaghen and C. Longeaud, in Proceedings of the 12th International Conference on Amorphous and Liquid Semiconductors [J. Non-Cryst. Solids **97&98**, 1059 (1987)].

[49]M. Stutzmann, W. B. Jackson, and C. C. Tsai, J. Non-Cryst. Solids **77&78**, 363 (1985).

[50]T. Shimizu, M. Kumeda, A. Morimoto, Y. Tsujimura, and I. Kobayashi, in *Materials Research Society Symposia Proceedings,* edited by D. Adler, Y. Hamakawa, and A. Madan (Materials Research Society, Pittsburgh, 1986), Vol. 70, p. 313.

[51]R. L. Weisfield, J. Appl. Phys. **54**, 6401 (1983).

[52]Speculations concerning the increase in GDOS, applicable to homogeneous material, have been discussed by G. Muller, Appl. Phys. A **45**, 103 (1988), in a paper published after the first submission of our article.

[53]E. A. Schiff, Philos. Mag. Lett. **55**, 87 (1987).

[54]See, for instance, R. Carius and W. Fuhs, in *Optical Effects in Amorphous Semiconductors (Snowbird, Utah),* Proceedings of the International Topical Conference on Optical Effects in Amorphous Semiconductors, AIP Conf. Proc. No. 120, edited by P. C. Taylor and S. G. Bishop (AIP, New York, 1984); F. Boulitrop, *ibid.*, p. 178.

[55]See, for instance, G. Moddel, Ph.D. thesis, Harvard University, 1981, and R. L. Weisfield, J. Appl. Phys. **54**, 6401 (1983).

[56]S. Guha, J. A. Payson, S. C. Agarwal, and S. R. Ovshinsky, in Proceedings of the 12th International Conference on Amorphous and Liquid Semiconductors [J. Non-Cryst. Solids **97&98**, 1455 (1987)].

[57]R. A. Street, J. C. Knights, and D. K. Biegelsen, Phys. Rev. B **18**, 1880 (1978).

[58]S. Oda, Y. Yamaguchi, J. Hanna, S. Ishihara, R. Fujiwara, S. Kawate, and I. Shimizu, in Technical Digest of the International PVSEC-1 (Kobe, 1984), p. 429.

[59]S. Guha (private communication).

[60]S. Wagner (private communication).

[61]S. R. Ovshinsky and D. Adler, in *Materials Research Society Symposia Proceedings,* edited by D. Adler, A. Madan, and M. J. Thompson (Materials Research Society, Pittsburgh, 1985), Vol. 49, p. 251.

[62]R. Weil, I. Abdulhalim, R. Beserman, M. Janai, and B. Pratt, J. Non-Cryst. Solids **77&78**, 261 (1985).

[63]Hydrogen evolution measurements carried out at Harvard by F. Moraes and S. J. Jones (unpublished). See also work on hydride-derived alloys by D. K. Paul, B. von Roedern, S. Oguz, J. Blake, and W. Paul, J. Phys. Soc. Jpn. Suppl. A **49**, 1261 (1980), and W. Beyer, H. Wagner, and F. Finger, J. Non-Cryst. Solids **77&78**, 857 (1985).

[64]S. Aljishi, D. S. Shen, V. Chu, Z. E. Smith, J. P. Conde, J. Kolodzey, D. Slobodin, and S. Wagner, in *Materials Research Society Symposia Proceedings,* edited by D. Adler, Y. Hamakawa, A. Madan, and M. Thompson (Materials Research Society, Pittsburgh, 1987), Vol. 95, p. 323.

[65]D. Slobodin, S. Aljishi, Y. Okada, D. S. Shen, V. Chu, and S. Wagner, in *Materials Research Society Symposia Proceedings,* edited by D. Adler, Y. Hamakawa, and A. Madan (Materials Research Society, Pittsburgh, 1986), Vol. 70, p. 275.

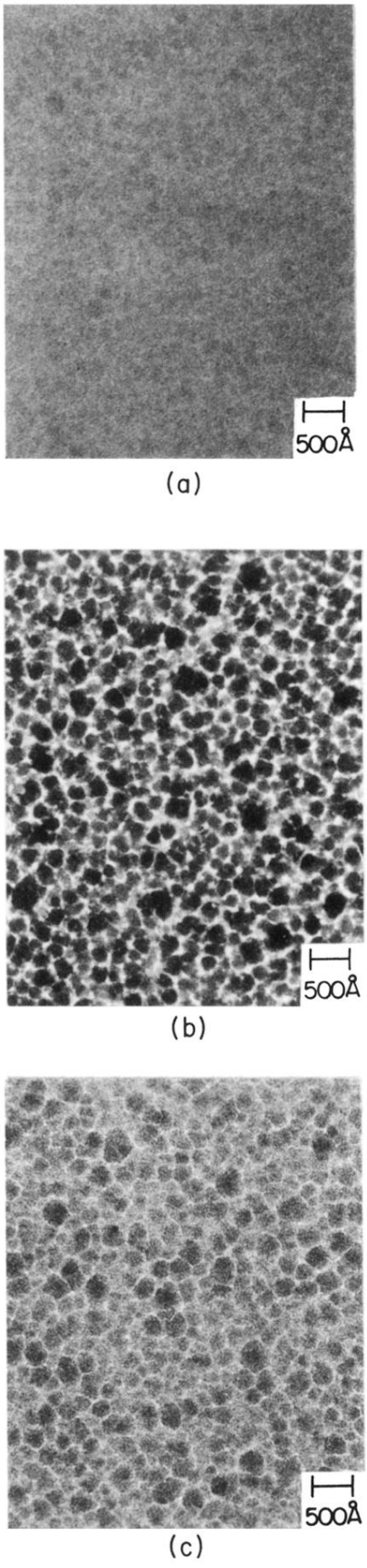

FIG. 16. Bright-field TEM images of (a) *a*-Si:H, (b) *a*-Ge:H, and (c) *a*-$Si_{0.5}Ge_{0.5}$:H. The specimens were prepared at substrate temperatures near 230 °C and are about 50 nm thick.

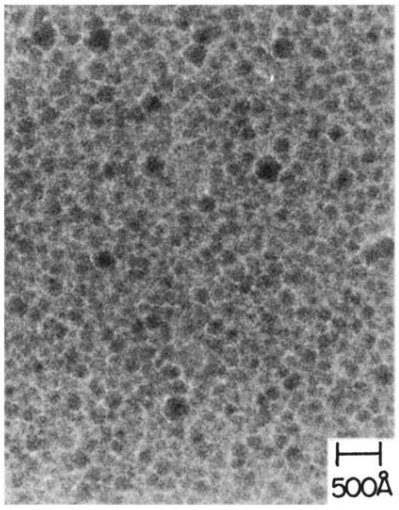

(a)

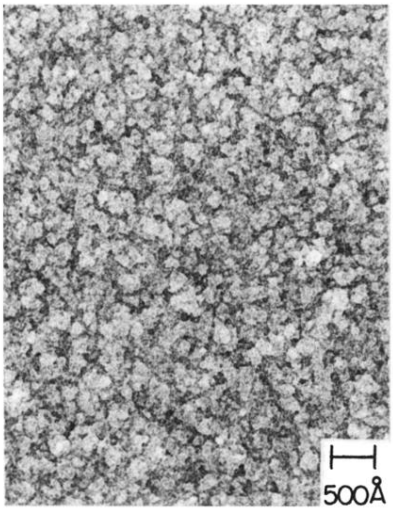

(b)

FIG. 17. Comparison of bright-field TEM images of (a) *a*-$Si_{0.5}Ge_{0.5}$:H, and (b) *a*-$Si_{0.5}Ge_{0.5}$:H:F. The specimens were prepared at 300 °C and are about 50 nm thick.